Research Article | Vol. 25, No. 5 | 6 Mar 2017 | OPTICS EXPRESS 4672

Optics EXPRESS

# All-optical guided-wave random laser in nematic liquid crystals

SREEKANTH PERUMBILAVIL,[1] ARMANDO PICCARDI,[2] OLEKSANDR BUCHNEV,[3] MARTTI KAURANEN,[1] GIUSEPPE STRANGI[4] AND GAETANO ASSANTO[1,2,*]

[1]*Photonics Laboratory, Tampere University of Technology, FI-33101 Tampere, Finland*
[2]*NooEL - Nonlinear Optics and OptoElectronics Lab, University "Roma Tre", I-00146 Rome, Italy*
[3]*Optoelectronics Research Centre, University of Southampton, SO17 1BJ, Southampton, United Kingdom* [4]*Dept. of Physics, Case Western Reserve University, Cleveland, Ohio 44106-7079, USA*
[*]*assanto@uniroma3.it*

**Abstract:** Spatial solitons can affect and enhance random lasing in optically-pumped dye-doped nematic liquid crystals. Upon launching two collinear beams in the sample, the first to pump the fluorescent guest molecules and the second to induce a reorientational soliton, strikingly the second beam not only guides the emitted photons in the soliton waveguide, but also enhances the lasing efficiency and modulates its spectral width. By altering the scattering paths of the emitted photons, the soliton also contributes to the selection of the lasing modes, as further confirmed by the observed kinks in the input/output characteristics. These experimental results demonstrate that random lasing can be efficiently controlled by a light beam which does not interact with the gain molecules, opening a route towards light-controlled random lasers.



**OCIS codes:** (190.5940) Self-action effects; (190.6135) Spatial solitons; (160.3380) Laser materials; (160.3710) Liquid crystals.

## References and links

1. H. Cao, "Lasing in random media," Waves Random Media **13** (3), R1–R39 (2003).
2. V. S. Letokhov, "Generation of light by a scattering medium with negative resonance absorption," Sov. Phys. JETP **26**, 835 (1968).
3. N. M. Lawandy, R. M. Balachandran, A. S. L. Gomes, and E. Sauvain, "Laser action in strongly scattering media," Nature **36**, 436–438 (1994).
4. D. S. Wiersma, "The physics and applications of random lasers," Nat. Phys. **4** (10), 359–367 (2008).
5. H. Cao, J. Y. Xu, D. Z. Zhang, S.-H. Chang, S. T. Ho, E. W. Seelig, X. Liu, and R. P. H. Chang, "Spatial confinement of laser light in active random media," Phys. Rev. Lett. **84**, 5584–5587 (2000).
6. M. Leonetti and C. Lopez, "Active subnanometer spectral control of a random laser," Appl. Phys. Lett. **102**, 071105 (2013).
7. M. Pang, X. Bao, L. Chen, Z. Qin, Y. Lu, and P. Lu, "Frequency stabilized coherent Brillouin random fiber laser: theory and experiments," Opt. Express **21** (22), 27155–27168 (2013).
8. R. C. Polson and Z. V. Vardeny, "Random lasing in human tissues," Appl. Phys. Lett. **85** (7), 1289–1291 (2004).
9. G. Strangi, S. Ferjani, V. Barna, A. De Luca, C. Versace, N. Scaramuzza, and R. Bartolino, "Random lasing and weak localization of light in dye-doped nematic liquid crystals," Opt. Express **14** (17), 7737–7744 (2006).
10. D. S. Wiersma and S. Cavalieri, "Light emission: a temperature-tunable random laser," Nature **414**, 708–709 (2001).
11. S. M. Morris, D. J.Gardiner, M. M. Qasim, P. J. W. Hands, T. D. Wilkinson, and H. J. Coles, "Lowering the excitation threshold of a random laser using the dynamic scattering states of an organosiloxane smectic A liquid crystal," J. Appl. Phys. **111**, 033106 (2012).
12. S. Mujumdar, S. Cavalieri, and D. S. Wiersma, "Temperature-tunable random lasing: numerical calculations and experiments," J. Opt. Soc. Am. B **21** (1), 201–207 (2004).
13. T. Nakamura, B. P. Tiwari, and S. Adachi, "Control of random lasing in $ZnOAl_2O_3$ nanopowders," Appl. Phys. Lett. **99**, 231105 (2011).
14. X. H. Wu, A. Yamilov, H. Noh, H. Cao, E. W. Seelig, and R. P. H. Chang, "Random lasing in closely packed resonant scatterers," J. Opt. Soc. Am. B **21** (1), 159–167 (2004).
15. S. Gottardo, S. Cavalieri, O. Yaroshchuk, and D. S. Wiersma, "Quasi-two-dimensional diffusive random laser action," Phys. Rev. Lett. **93**, 263901 (2004).
16. N. Bachelard, J. Andreasen, S. Gigan, and P. Sebbah, "Taming random lasers through active spatial control of the pump," Phys. Rev. Lett. **109**, 033903 (2012).

#283534 https://doi.org/10.1364/OE.25.004672
Journal © 2017 Received 22 Dec 2016; revised 2 Feb 2017; accepted 15 Feb 2017; published 21 Feb 2017

Optics EXPRESS

17. H. Cao, Y. G. Zhao, S. T. Ho, E. W. Seelig, Q. H. Wang, and R. P. H. Chang, "Random laser action in semiconductor powder," Phys. Rev. Lett. **82**, 2278–2281 (1999).
18. S. Mujumdar, M. Ricci, R. Torre, and D. S. Wiersma, "Amplified extended modes in random lasers," Phys. Rev. Lett. **93**, 053903 (2004).
19. M. Leonetti, C. Conti, and C. Lopez, "The mode locking transition of random lasers," Nat. Photonics **5**, 615–617 (2011).
20. P. G. DeGennes and J. Prost, *The Physics of Liquid Crystals* (Oxford Science, 1993).
21. I. C. Khoo, *Liquid Crystals: Physical Properties and Nonlinear Optical Phenomena* (Wiley, 1995).
22. S. Ferjani, V. Barna, A. De Luca, C. Versace, N. Scaramuzza, R. Bartolino, and G. Strangi, "Thermal behavior of random lasing in dye-doped nematic liquid crystals," Appl. Phys. Lett. **89**, 121109 (2006).
23. M. Peccianti and G. Assanto, "Nematicons," Phys. Rep. **516**, 147–208 (2012).
24. M. Peccianti, C. Conti, G. Assanto, A. De Luca, and C. Umeton, "Routing of anisotropic spatial solitons and modulational instability in nematic liquid crystals," Nature **432**, 733 (2004).
25. M. Warenghem, J.F. Henninot, and G. Abbate, "Non linearly induced self waveguiding structure in dye doped nematic liquid crystals confined in capillaries," Opt. Express **2** (12), 483–490 (1998).
26. J. Beeckman, K. Neyts, X. Hutsebaut, C. Cambournac, and M. Haelterman, "Simulations and experiments on self-focusing conditions in nematic liquid-crystal planar cells," Opt. Express. **12**(6), 1011–1018 (2004).
27. M. Peccianti, G. Assanto, A. De Luca, C. Umeton, and I. C. Khoo, "Electrically assisted self-confinement and waveguiding in planar nematic liquid crystal cells," Appl. Phys. Lett. **77**(1), 7–9 (2000).
28. G. Assanto, A. Fratalocchi, and M. Peccianti, "Spatial solitons in nematic liquid crystals: from bulk to discrete," Opt. Express **15**(8), 5248–5259 (2007)
29. Y. V. Izdebskaya, V. G. Shvedov, A. S. Desyatnikov, W. Z. Krolikowski, M. BeliÄĞ, G. Assanto, and Y. S. Kivshar, "Counterpropagating nematicons in bias-free liquid crystals ," Opt. Express **18**(4), 3258-3263 (2010).
30. A. Alberucci, A. Piccardi, M. Peccianti, M. Kaczmarek, and G. Assanto, "Propagation of spatial optical solitons in a dielectric with adjustable nonlinearity," Phys. Rev. A **82**(2), 023806 (2010).
31. A. Piccardi, A. Alberucci, and G. Assanto, "Self-turning self-confined light beams in guest-host media," Phys. Rev. Lett. **104**, 213904 (2010).
32. J. F. Henninot, J. F. Blach, and M. Warenghem, "Enhancement of dye fluorescence recovery in nematic liquid crystals using a spatial optical soliton," J. Appl. Phys. **107**, 113111 (2010).
33. S. Bolis, T. Virgili, S. K. Rajendran, J. Beeckman, and P. Kockaert, "Nematicon-driven injection of amplified spontaneous emission into an optical fiber," Opt. Lett. **41**(10), 2245–2248 (2016).
34. I. Burgess, M. Peccianti, G. Assanto, and R. Morandotti, "Accessible light bullets via synergetic nonlinearities," Phys. Rev. Lett. **102**, 203903 (2009).
35. M. Peccianti, A. Pasquazi, G. Assanto, and R. Morandotti, "Enhancement of third-harmonic generation in nonlocal spatial solitons," Opt. Lett. **35**(20), 3342–3344 (2010).
36. U. A. Laudyn, M. Kwasny, A. Piccardi, M. A. Karpierz, R. Dabrowski, O. Chojnowska, A. Alberucci, and G. Assanto, "Nonlinear competition in nematicon propagation," Opt. Lett. **40**(22), 5235–5238 (2015).
37. J. Yi, Y. Yu, J. Shang, X. An, B. Tu, G. Feng, and S. Zhou, "Waveguide random laser based on a disordered ZnSe-nanosheets arrangement," Opt. Express **24**(5), 5102–5109 (2016).
38. S. Perumbilavil, A. Piccardi, O. Buchnev, M. Kauranen, G. Strangi, and G. Assanto, "Soliton-assisted random lasing in optically-pumped liquid crystals," Appl. Phys. Lett. **102**, 203903 (2016).
39. E. Yariv and R. Reisfeld, "Laser properties of pyrromethene dyes in sol-gel glasses," Opt. Mater. **13**, 49 (1999).
40. J. H. Lin, Y. L. Hsiao, B. Y. Ciou, S. H. Lin, Y. H. Chen, and J. J. Wu, "Manipulation of random lasing action from dye-doped liquid crystals infilling two-dimensional confinement single core capillary," IEEE Photonics J. **7**(3), 1501809 (2015).
41. I. Jánossy and T. Kósa, "Influence of anthraquinone dyes on optical reorientation of nematic liquid crystals," Opt. Lett. **17**(17), 1183–1185 (1992).
42. L. Sznitko, K. Kaliciak, A. Adamow, and J. Mysliwiec, "A random laser made of nematic liquid crystal doped with a laser dye," Opt. Mat. **56**, 121–128 (2016).
43. T. Nakamura, S. Sonoda, T. Yamamoto, and S. Adachi, "Discrete-mode ZnO microparticle random laser," Opt. Lett. **40**(11), 2661–2664 (2015).
44. B. He, Q. Liao, and Y. Huang, "Random lasing in a dye doped cholesteric liquid crystal polymer solution," Opt. Mat. **31**, 375–379 (2008).
45. G. van Soest and A. Lagendijk, "Beta factor in a random laser," Phys. Rev. E **65**, 047602 (2002).

## 1. Introduction

Random lasing occurs when disorder in an optically amplifying medium provides multiple scattering events for emitted light, such that the resulting photon paths allow for amplification and stimulated emission, even in the absence of an actual cavity [1]. Since its prediction [2] and the first experimental demonstration [3], several efforts were devoted to obtaining random lasing

Optics EXPRESS

(RL), foreseeing the development of low cost coherent sources [4]. To achieve random lasing, the significant scattering required from the active medium or the host was obtained in powders [3,5,6], optical fibers [7], biological tissues [8] and liquid crystals [9–11]. At the same time, the strong dependence of RL emission on environmental parameters offered unprecedented opportunities to tune the lasing properties through, e.g., temperature control [12], concentration of active molecules in host materials [13], grain size in powder systems [14], bias voltage [11, 15], spatial profile of the pump beam [6, 16]. By acting on the favoured scattering paths (equivalent to tuning the cavity in standard lasers), it was possible to select lasing modes [17, 18] and lock them [19].

Liquid crystals are mesophases possessing a finite degree of positional and/or orientational order, due to their relatively weak intermolecular links [20]. In the nematic phase the positional order is negligible, while the long axes of the oriented molecules are aligned in an average direction, termed molecular director **n** and corresponding to the optic axis of the macroscopic uniaxial material [21]. RL can be obtained in nematic liquid crystals (NLC) by doping them with a pump-resonant active dye, as demonstrated in various systems [9, 22]. The director distribution in NLC can be adjusted by the application of electric fields [15], making them excellent candidates for the tuning of random lasers.

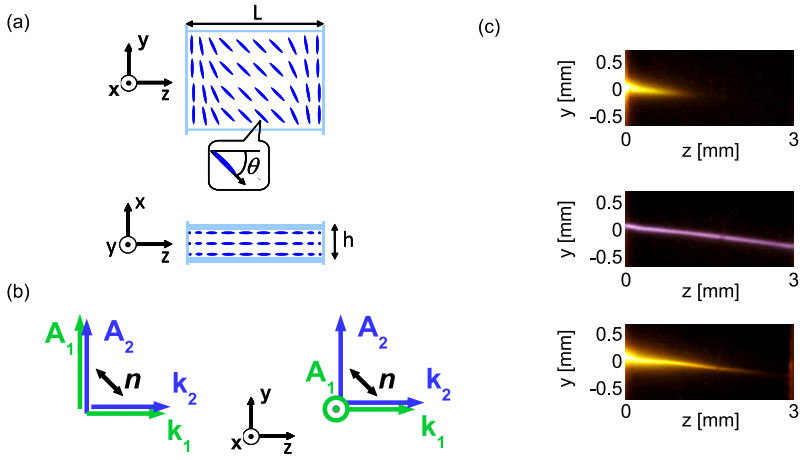


Fig. 1. (a) Sketch of the planar NLC sample. (b) Launch geometries in the principal plane $yz$, with $A_1$ and $A_2$ the amplitudes of the visible pump beam and the near-infrared solitary beam, respectively. (c) Acquired photographs of fluorescence emitted *e*-wave photons without nematicon (top), near-infrared nematicon (center), emitted *e*-wave light in the presence of a co-polarized nematicon (bottom). The near-infrared was filtered out in the last case.

Another important property of NLC is their nonlinear optical response, with a dominant contribution from molecular reorientation through the torque provided by the electric field of light on the dipoles induced in the elongated molecules. When all-optical reorientation is produced by a finite size beam, the corresponding increase in refractive index for extraordinarily polarized waves leads to self-focusing and eventually self-confinement, with the propagation of an optical spatial soliton and the formation of a light-induced waveguide [23]. Spatial solitons and their control in nematic liquid crystals ("nematicons") have been extensively reported in the past two decades [23–31]; they form when a finite beam produces a graded director distribution and refractive index profile with self-focusing balancing out linear diffraction [23]. Such light-induced waveguides can confine co-polarized signals at other wavelengths [27], as well as light emitted through fluorescence or spontaneous emission [31–33]; moreover, distinct regimes allow for

Optics EXPRESS

the effective synergy of diverse nonlinear responses in NLC and their mutual control in the presence of solitons [34–36]. In this work we control the RL emission of a planar dye-doped NLC sample exploiting all-optical reorientation to launch a soliton at a wavelength well removed from the guest-host absorption resonance. We demonstrate that, in analogy to other guiding geometries [37], the light-induced waveguide associated to a soliton can confine the emitted photons in the extraordinary polarization [33, 38], enhancing the overall lasing efficiency. This approach to random lasing, combining a resonant light-matter interaction between the pump and the guest-host with a non-resonant one supporting beam self-confinement via reorientation, can be exploited for a novel generation of controllable cavity-less lasers.

## 2. Experimental setup and sample characterization

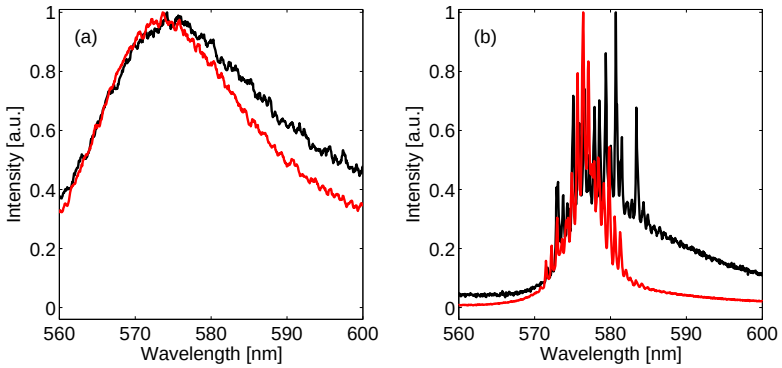


Fig. 2. (a) Typical examples of normalized spectra below lasing threshold, for an input pump beam polarized along $x$ and energy $E = 0.6\mu$J, without (black line) and with (red line) a collinear 6mW nematicon. (b) Same as in (a) but above threshold at a pump energy $E = 1\mu$J.

The sample we used in the experiments, sketched in Fig. 1(a) and similar to that previously used, e.g., in [24, 33, 38], consists of two parallel glass slides separated by Mylar spacers, surface treated with polyimide to favor the NLC alignment at $\theta = \angle \mathbf{n}\hat{z} = \pi/4$, thus maximizing the birefringent walkoff of the equivalent uniaxial and the nonlinearity experienced by an extraordinary -wave (*e*-) beam propagating with $\mathbf{k}$ parallel to $\hat{z}$ [30]. Two other thinner glass interfaces perpendicular to $z$ seal the cell and provide anchoring with $\mathbf{n}$ parallel to $y$ in order to optimize the coupling of radiation (input laser beam) into the extraordinary wave [24]. The cell is infiltrated by capillarity with a mixture of the commercial E7 NLC with a 0.3wt% of Pyrromethene dye (PM597). The latter dye is based on the fluoroboration of two pyrrole rings linked by a conjugated $\pi$-system chain, yielding the dipyrromethene-BF2 complexes also known as cyclic cyanine dyes; it has a fluorescence quantum yield approaching unity and can lase more efficiently than other common dyes such as rhodamine, also because of the low T-T absorption capacity over the lasing spectrum [9, 39]. A similar mixture, with absorption peaked around 530nm, has been demonstrated to random lase in various configurations (wedge cells, drops, capillaries) and allow for temperature tuning [9, 22, 40]. It has been proven that the optically-induced molecular reorientation for wavelengths out of the dye absorption band is not affected by such a low concentration of fluorescent guest molecules in the nematic host [41]. Thus, PM597-E7 is an excellent guest-host system to investigate the interplay between the pumping beam and the reorienting beam for conveying all-optically controlled random laser emission.

We employed two laser beams of different intensities and wavelengths to independently excite the two nonlinear mechanisms, namely fluorescence/lasing and reorientation, focusing

Optics EXPRESS

them at the cell entrance through a microscope objective and additional optics to obtain comparable waists $w_0 \approx 4\mu$m at the input facet. A microscope imaged the out-of-plane scattered light into a CCD camera, allowing for the acquisition of beam evolution in the principal propagation plane $yz$. At the output, a spectrometer equipped with a 100$\mu$m-core multimode fiber and a 100$\mu$m slit collected the emitted light and acquired the spectra. A continuous-wave near-infrared (NIR) $y$-polarized Gaussian beam at $\lambda = 1.064\mu$m was launched in the cell to excite a nematicon at powers $P > 2$mW, propagating with a transverse angular velocity (walkoff) $\delta = \arctan[\epsilon_a \sin 2\theta/(\epsilon_a + 2n_\perp^2 + \epsilon_a \cos 2\theta)]$ with respect to the wavevector (**k** parallel to $\hat{z}$) [24], according to the initial director alignment, with $\epsilon_a = n_\parallel^2 - n_\perp^2 > 0$ the optical anisotropy ($n_\parallel$ and $n_\perp$ being the refractive indices for fields parallel and orthogonal to the optic axis, respectively). We generated fluorescence and RL emission with a frequency-doubled Q-switched 6ns-pulse Nd:YAG source at wavelength 532nm and 20Hz repetition rate.

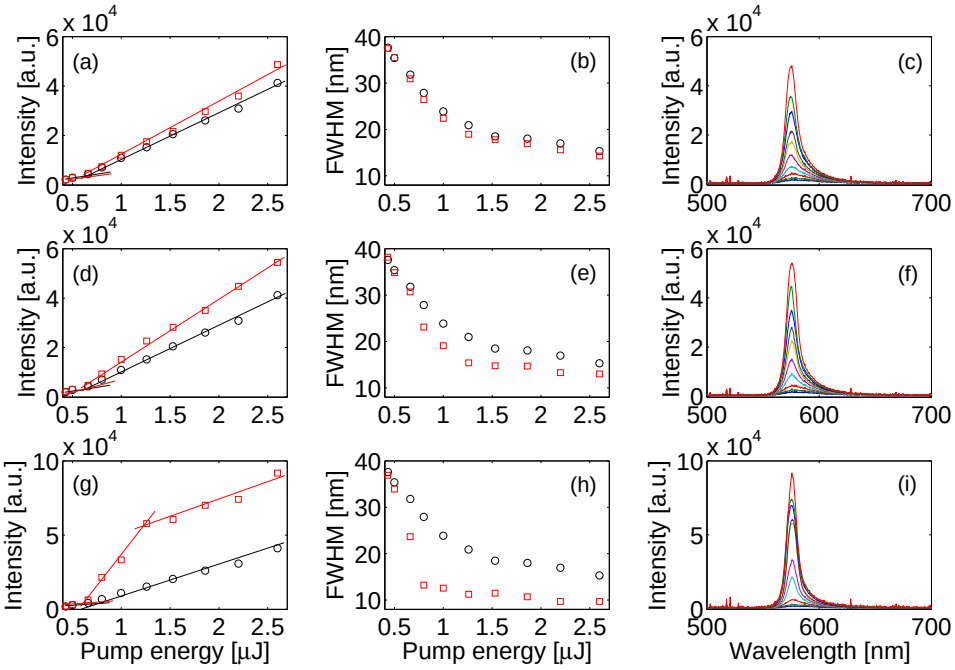


Fig. 3. (a)-(d)-(g) Input/output random lasing characteristics and (b)-(e)-(h) emission spectrum full-widths at half-maximum (FWHM) versus pump energy/pulse; (c)-(f)-(i) Emission spectra versus wavelength at the used pump energies. (a-c) Results for the interaction between RL and a $P_{NIR} = 2m$W nematicon (red symbols and line) compared to the case without nematicon (black symbols and line): the soliton waveguide marginally affects RL emission. (d-f) Same as (a-c), but for $P_{NIR} = 6$mW: the NIR-induced confinement enhances RL, with a higher gain accompanied by spectral narrowing. (g-i) Same as (a-c), for $P_{NIR} = 14$mW: the spectra further narrow down and a kink appears in the input/output characteristic (g). Narrower profiles in (c)-(f)-(i) correspond to increasing pump energies.

The spectra obtained by pumping the material (in the absence of a NIR nematicon) with either **k** along $\hat{x}$ (transverse geometry) or **k** parallel to $\hat{z}$ in the $yz$ plane (principal plane of the NIR beam) exhibited RL emission peaked around 576nm, non-collinear to the pump beam owing to the optical anisotropy and to the randomness of the resonant feedback [9, 15]. Since

Optics EXPRESS

material anisotropy affects both the lasing efficiency and the emission polarization [15, 42], the emitted light was an *e*-wave in the plane $\mathbf{n}\hat{z} \equiv \hat{y}\hat{z}$ despite the pump polarization, whereas the emission efficiency was maximum for a pump *x*-polarized perpendicular to the director, as previously reported in [38] but at variance with [9]. This polarization dependence suggests that the combined action of the two beams can yield efficient RL for an ordinary-wave (*o*-) pump collinear with the *e*-wave soliton (Fig. 1(b), right), allowing the latter to confine the emitted light in the waveguide region if a suitable input tilt compensates for the limited beam overlap due to the angular walkoff of the soliton. The alternative configuration, an *e*-pump collinear with and confined by the *e*-soliton (Fig. 1(b),left), would maximize the overlap of pump and fluorescence in the nematicon region, but at the expenses of the resulting emission. Figure 1(c) shows the acquired pictures of (top) the emitted (green-yellow) photons, (middle) the NIR beam featuring self-confinement and (bottom) the emitted (*y*-polarized) photons guided by the nematicon waveguide.

## 3. Results and discussion

As described above, we co-launched two co-planar beams sharing one and the same direction of their Poynting vectors in the medium, an ordinary (*o*-) polarized pump (visible) and an *e*-wave nematicon (NIR), adjusting their waists and tilt in order to maximize the overlap between the emitted fluorescent light and the green pump within the graded-index waveguide formed by the NIR soliton. As we demonstrated earlier [38], light-induced reorientation alters the scattering paths of the emission and limits diffraction, beneficially affecting the random lasing characteristics. Typical emission spectra of the emitted light (single realizations) below and above lasing threshold are shown in Fig. 2 with and without the presence of a NIR nematicon collinear with the *o*-pump beam. To gain a better insight on the phenomenon, we acquired the input/output characteristics as well as the output spectra of the generated radiation as we varied both the pump pulse energy and the soliton power, as shown in Fig. 3 after averaging over numerous (> 60) pulse realizations and employing a spectrometer with limited resolution (≈nm) in order to present and compare smooth (realization-independent) profiles. As a result, Fig. 3 the FWHM values are overestimated.

For $P_{NIR}$ = 2mW nonlinear reorientation gives rise to an NIR spatial soliton but contributes negligibly to the overall RL performance, as apparent in Figs. 3(a)–(c): the RL spectra without (not shown) and with the nematicon exhibit marginal differences. Things change when the soliton power increases as, e.g., for $P_{NIR}$ = 6mW (Figs. 3(d)–(f)): soliton induced reorientation features a higher RL efficiency and lowers the $\beta$-factor (Fig. 3(d)), with a moderate narrowing of the emission spectra as compared to the bulk case without nematicon (Figs. 3(e)–(f)).

Further increases in soliton power allow to access a the RL regime illustrated, e.g., in Fig. 3(g): for $P_{NIR}$ = 14mW the input/output curve above threshold initially exhibits a higher gain, later followed by a reduced slope at energies above $E_k \approx 1.25\mu$J where a "kink" appears. Consistently with similar effects observed in other random lasing systems [43, 44], this behavior can be attributed to the interaction/competition of several lasing modes in the large interaction volume defined by the cell length L, with a resulting saturation of the laser gain.

Figure 4 collates RL input/output curves versus pump energy for various NIR soliton powers, up to $P_{NIR}$ = 18mW; at powers of 18mW and higher, nematicons tend to become less stable and exhibit trajectory fluctuations in the transverse plane. It is apparent that, although soliton-driven reorientation does not affect the RL threshold energy $E_{th} \approx 0.7\mu$J, the transition to lasing gets sharper and the slope of the laser intensity versus pump energy/pulse initially increases with $P_{NIR}$. The corresponding enhancement factors $\beta$, calculated from the emission spectra before (fluorescence) and after (RL) threshold at a pump energy $E = 1\mu$J according to [45], are indicated in the legend for various nematicon powers. Surprisingly, the kink remains approximately positioned at $E_k \approx 1.25\mu$J and it only appears in the presence of the nematicon, which is likely

Optics EXPRESS

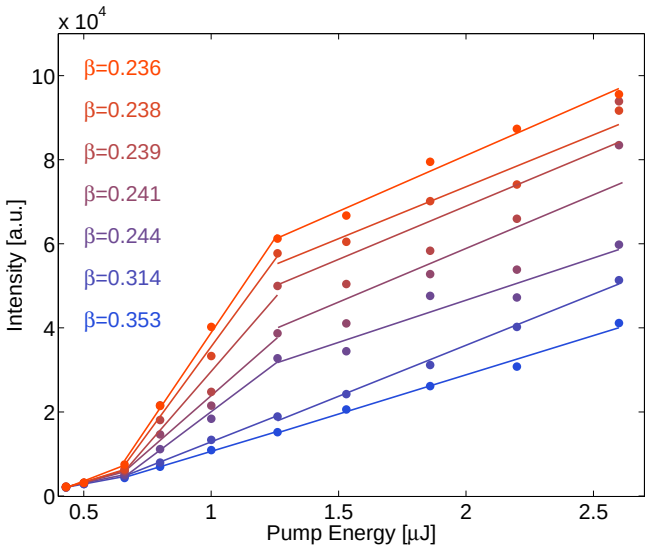


Fig. 4. Input/output random laser characteristics for various soliton powers, with the corresponding $\beta$-factors calculated at $E = 1\mu J$ and indicated in the legend. Neither the energy threshold nor the kink location change with nematicon power. From bottom to top the curves correspond to $P_{NIR} = 0, 2, 6, 10, 12, 14, 16, 18$mW, respectively.

to trigger a more efficient mode selection. A quantitative estimate of the interaction between the emitted photons and the pump, various scattering paths and their modulation by soliton reorientation, are beyond the scopes of this paper and will be discussed in future work together with a suitable model.

Figure 5 illustrates the role of nematicons on random lasing, graphing RL spectra for various nematicon powers, as well as the corresponding FWHM and the peak emitted intensities (as acquired by the spectrometer). At a pump energy $E \approx 0.66\mu J$ (Figs. 5(a) and 5(b)), below lasing threshold, the presence of a soliton collinear with the pump does not produce dramatic changes, with a moderate enhancement $G = \frac{I_{P_{Max}}}{I_{P=0}} \approx 2$ due to improved photon collection and a spectral narrowing $S_n = \left|\frac{(FWHM_{P_{Max}} - FWHM_{P=0})}{FWHM_{P=0}}\right| > 0.25$, as visible in Fig. 5(b). At energy $E = \approx 1.0\mu J$ (Figs. 5(c) and 5(d)), just above RL threshold, the gain enhancement is $G \approx 5$ with narrowing $S_n \approx 0.62$, i.e., FWHM dropping from 24 to $9nm$. Finally, at energy $E = 1.53\mu J$ above $E_k$ (Figs. 5(e) and 5(f)), $G \approx 8$ with $S_n \approx 0.55$.

## 4. Conclusions

We experimentally investigated the interaction between two nonlinear effects occurring in dye-doped nematic liquid crystals, namely random lasing in scattering media and beam self-confinement via a Kerr-like all-optical response. We demonstrated that an optical spatial soliton is able to modify the lasing properties of the strongly scattering random medium, altering the scattering paths and the resulting feedback available in the interaction volume. RL emission is assisted and enhanced by solitons through both light guiding and scattering modulation, resulting in gain enhancement, spectral narrowing and reduction in $\beta$-factor, mode selection and, eventually, kinks in the input/output characteristic. This report introduces a guest-host system where a passive nonlinear response (beam self-focusing and self-trapping) acts in synergy with an active mechanism (optical gain and laser action) to yield all-optical control of random las-

Optics EXPRESS

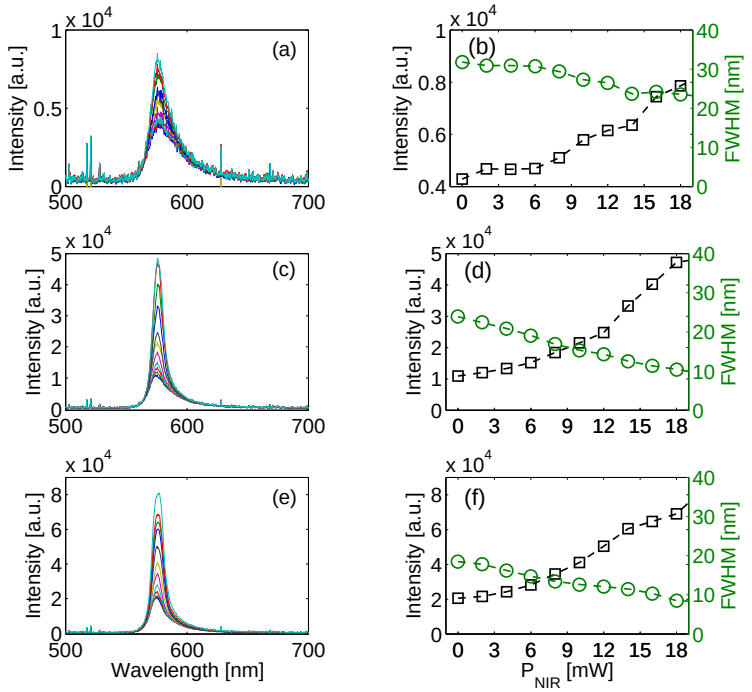


Fig. 5. Soliton assisted RL enhancement. (a) Emission spectra for nematicon powers from $P_{NIR}$ = 0mW (broadest) to $P_{NIR}$ = 18mW (narrowest) and (b) corresponding FWHM (circles) and peak emission intensity (squares) versus soliton power $P_{NIR}$, for a pump energy $E = 0.66\mu$J below threshold. (c-d) As in (a-b) but for $E = 1\mu$J, above threshold. (e-f) As in (a-b) or $E = 1.53\mu$J, above the kink in Fig. 4.

ing in the presence of strong disorder. Among the several advantages illustrated above with these preliminary data, we pinpoint light-controlled emission using beams of different wavelengths and intensities, an extended interaction volume with a large number of lasing modes, power-controlled gain enhancement as well as spectral narrowing. Such features are promising towards the implementation of nonlinearly adjusted light sources and processors.

## Funding

Suomen Academy, Finland Distinguished Professor (282858); European Union (EU) COST action IC1208.

## Acknowledgments

We thank S. Bolis for useful discussions and Dr. R. Barboza for precious suggestios and invaluable help with the experiments. S.P., A.P. and G.A. acknowledge the Academy of Finland for support through the FiDiPro grant no. 282858.